

# Spin-orbit interaction of light and diffraction of polarized beams

Aleksandr Ya. Bekshaev

Odessa I.I. Mechnikov National University  
Dvorianska 2, 65082 Odessa, Ukraine  
E-mail: bekshaev@onu.edu.ua

The edge diffraction of a paraxial vector light beam is studied theoretically based on the Fresnel-Kirchhoff approximation, and the dependence of the diffracted beam pattern of the incident beam polarization is predicted. If the incident beam is circularly polarized, the trajectory of the diffracted beam centre of gravity experiences a small angular deviation from the geometrically expected direction. The deviation is parallel to the screen edge and reverses the sign with the polarization handedness; it is explicitly calculated for the case of a Gaussian incident beam with plane wavefront. This effect is a manifestation of the spin-orbit interaction of light and can be interpreted as a revelation of the internal spin energy flow immanent in circularly polarized beams. It also exposes the vortex character of the weak longitudinal field component associated with the circularly polarized incident beam.

Keywords: spin-orbit interaction, spin Hall effect of light, vector beams, diffraction, spin momentum, optical vortex

## 1. Introduction

Apparently, evolution of propagating light beams is performed independently of its polarization: the spatial and polarization degrees of freedom are separated. However, a more detailed investigation reveals that the polarization state affects the propagating beam spatial pattern; the corresponding effects, generally rather fine and only observable under special conditions, are known as manifestations of the spin-orbit interaction (SOI), or spin-orbit coupling of light [1–18]. In many cases, SOI takes place in presence of inhomogeneous or anisotropic media and are mediated by the light–matter interaction [5–13]; however, even the free space transformation demonstrates distinct polarization-dependent features [14–18]. Among diverse manifestations of the SOI, the special place belongs to the spin Hall effect (SHE) of light – a polarization-induced transverse shift of the beam trajectory. Usually it is expressed by the fact that the “center of gravity” (CG) of the transverse energy distribution in the beam slightly deviates from the geometric expectations, depending on the handedness of the beam circular polarization [5–17]. There are different versions of this phenomenon; it can be associated with the strong inhomogeneity occurring, e.g., at a plane boundary between different optical media [6–11], or may evolve gradually during the beam propagation through an inhomogeneous medium [1,5,12]. The most impressive are the SOI manifestations observable in freely propagating optical fields

(in particular, upon tight focusing of a perturbed Gaussian beam with broken circular symmetry [14–16]).

Many features of the SHE show a remarkable analogy with the phenomena typical to the orbit-orbit coupling (interaction between the intrinsic and extrinsic spatial degrees of freedom) of light [19–23]. According to [21,23], the “orbital” Hall effect of light appears as an external manifestation of the internal energy circulation existing in the beams with optical vortices and characterized by the intrinsic orbital angular momentum (OAM) of such beams. The mentioned analogy inspires the search for similar energy-flow mechanisms underlying the SHE [23,24].

It should be emphasized that the orbit-orbit coupling effects have proven their value as means for the energy circulation detection and diagnostics. These are especially impressive in cases of optical vortex (OV) beam diffraction [4,25–32] where the diffracted beam evolution behind the diffraction screen spectacularly exposes the presence of the transverse energy circulation and enables to determine some of its quantitative parameters.

Actually, the circulatory energy flow also exists in non-vortex beams with regular structure (e.g., Gaussian ones) provided that they are elliptically or circularly polarized [4]. This is the “spin flow” associated with the spin, or Belinfante’s momentum [33–37]. The handedness and intensity of this ‘spin’ circulation are dictated by the polarization handedness and the beam amplitude inhomogeneity (an example of the spin flow distribution within the cross section of a circularly polarized Gaussian beam is schematically shown in figure 1). Sometimes the spin flow is considered ‘virtual’ as it causes no real energy transfer; at the same time, it is the source of the spin angular momentum (SAM) of elliptically polarized beams and provides an articulate mechanical action [34] due to which it can be experimentally detected and measured [38]. Keeping in mind the mentioned analogy between the SOI and orbit-orbit interaction, it is tempting to look for specific SHE versions in which the circulatory spin flow manifests itself in a manner similar to how the orbital energy circulation “comes to light” in the edge diffraction of beams with OAM. In a word, it is quite expectable that diffraction of a circularly polarized beam with the SAM depends on the polarization handedness, and the latter can be deduced from the diffraction pattern, just as the sign of OAM can be deduced from the diffraction of OV beams. In this paper, we theoretically verify this hypothesis and develop its simple quantitative estimations.

## 2. Diffraction model

In figure 1, the usual scheme of the edge diffraction is presented [29–31]. Our subject is the paraxial monochromatic (wavenumber  $k$ ) beam propagating along axis  $z$ , that diffracts at the rectilinear edge of the opaque screen situated in the plane  $z = 0$ . The beam electromagnetic field can be represented as a superposition of  $x$ - and  $y$ -polarized components with electric and magnetic vectors [4,10,33]

$$\begin{aligned} \begin{Bmatrix} \mathbf{E}_x \\ \mathbf{H}_x \end{Bmatrix} &= \exp(ikz) \left( \begin{Bmatrix} \mathbf{e}_x \\ \mathbf{e}_y \end{Bmatrix} u_x + \frac{i}{k} \mathbf{e}_z \begin{Bmatrix} \partial/\partial x \\ \partial/\partial y \end{Bmatrix} u_x \right), \\ \begin{Bmatrix} \mathbf{E}_y \\ \mathbf{H}_y \end{Bmatrix} &= \exp(ikz) \left( \begin{Bmatrix} \mathbf{e}_y \\ -\mathbf{e}_x \end{Bmatrix} u_y + \frac{i}{k} \mathbf{e}_z \begin{Bmatrix} \partial/\partial y \\ -\partial/\partial x \end{Bmatrix} u_y \right) \end{aligned} \quad (1)$$

where  $u_j$  are the slowly varying complex amplitudes,  $\mathbf{e}_j$  are the unit vectors of the coordinate axes ( $j = x, y, z$ ). Note that in contrast to the previously considered scalar model of diffraction [29–31], now we deal with the vector beam field whose characteristic feature is the non-zero longitudinal components  $E_z = \exp(ikz)v_z$ ,  $H_z = \exp(ikz)v_{Hz}$  with complex amplitudes

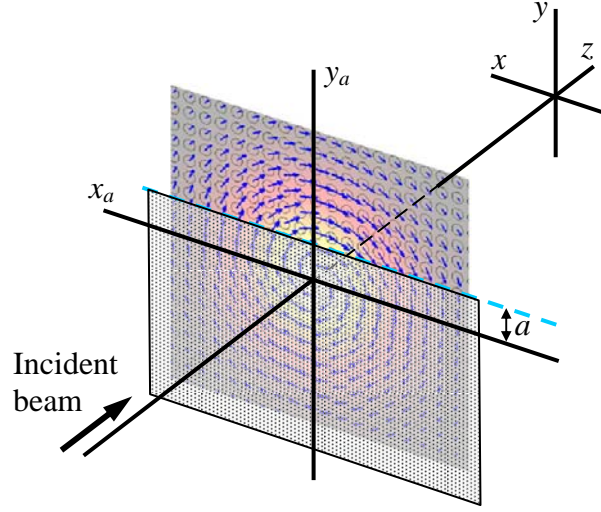


**Figure 1.** Scheme illustrating the geometrical conditions of diffraction. The opaque screen (conventionally shown as semitransparent) covers the lower part of the beam cross section ( $y < a$  half-plane). The incident beam is Gaussian and circularly polarized ( $\sigma = +1$ ), the spin flow lines and the polarization ellipses (circles) are shown over the intensity distribution (color-coded background). The diffracted beam is observed at a distance  $z$  behind the screen.

$$v_z = \frac{i}{k} \left( \frac{\partial u_x}{\partial x} + \frac{\partial u_y}{\partial y} \right), \quad v_{Hz} = \frac{i}{k} \left( -\frac{\partial u_y}{\partial x} + \frac{\partial u_x}{\partial y} \right). \quad (2)$$

Within the frame of the paraxial approximation, the longitudinal field (2) is small in respect to the transverse field,  $v_z \sim \gamma(u_x, u_y)$ , where the small parameter  $\gamma$  coincides with the angle of self-diffraction (beam divergence) [4,33]. In further reasoning we will deal mainly with the electric field, keeping in mind that in case of necessity the magnetic field characteristics can be easily obtained via equations (1), (2).

To make the analysis more direct, we just take the most interesting case when the incident beam is homogeneously circularly polarized, that is, for  $z < 0$

$$u_y = i\sigma u_x \quad (3)$$

where  $\sigma = \pm 1$  is the polarization handedness. Also, we suppose that the beam is axially symmetric with respect to  $z$ :

$$u_x(x, y, z) = u_x(r, z), \quad \frac{\partial u_x}{\partial \phi} \equiv 0 \quad (z < 0) \quad (4)$$

where the polar coordinates  $(r, \phi)$  are introduced via the usual definitions

$$x = r \cos \phi, \quad y = r \sin \phi.$$

Under conditions (3) and (4), the complex amplitudes of the longitudinal field accept the form

$$v_z = \frac{i}{k} \exp(i\sigma\phi) \frac{\partial u_x}{\partial r}, \quad v_{Hz} = -i\sigma v_z \quad (5)$$

which indicates its OV nature [4,10]. In this way, the analogy to the beams with OAM finds a distinct quantitative argument: at least the longitudinal component of the SAM-carrying beam (1)

contains a certain transverse energy circulation that should reveal itself in the edge-diffraction processes.

Now we consider the beam diffraction based on the standard scheme presented in figure 1 [29–31]. The diffracted field is calculated via the Fresnel-Kirchhoff integral [39]

$$u(x, y, z > 0) = \frac{k}{2\pi iz} \int_a^\infty dy_a \int_{-\infty}^\infty dx_a u(x_a, y_a, 0) \exp\left\{\frac{ik}{2z}[(x-x_a)^2 + (y-y_a)^2]\right\}. \quad (6)$$

where  $u(x_a, y_a, 0)$  is the incident beam complex amplitude in the screen plane. This equation is derived for the scalar field model and its application to vector beams needs some special remarks.

Usually it is applied to the transverse components that in the Kirchhoff approximation diffract independently (the small difference in the behavior of the field components parallel and orthogonal to the screen edge depends on the screen nature and is neglected). The longitudinal component can then be calculated via equations (2) (note that behind the screen, the beam is no longer axially symmetric). However, this way meets difficulties in finding the derivatives of discontinuous functions [29]: just after the screen,  $u_x$  and  $u_y$  sharply fall to zero at  $y = a$ . To avoid these difficulties, we consider the diffraction of the longitudinal component separately. Indeed, differentiating of equation (6) generates the quite similar relation for the complex amplitude derivatives, which immediately entails the same Fresnel-Kirchhoff integral for the longitudinal component:

$$v_z(x, y, z > 0) = \frac{k}{2\pi iz} \int_a^\infty dy_a \int_{-\infty}^\infty dx_a v_z(x_a, y_a, 0) \exp\left\{\frac{ik}{2z}[(x-x_a)^2 + (y-y_a)^2]\right\}. \quad (7)$$

### 3. Diffracted beam trajectory characterization

Thus, we have the sufficient apparatus for calculation of the whole diffracted beam field. However, we do not intend to study all details of the diffracted beam spatial pattern but rather to find the integral characteristic of its trajectory. As usual [14–16], we characterize the beam position by the CG of the transverse energy distribution

$$\mathbf{r}_c = \frac{\int \mathbf{r} w dx dy}{\int w dx dy} \quad (8)$$

where  $\mathbf{r} = \begin{pmatrix} x \\ y \end{pmatrix}$  is the transverse radius-vector; from now on, absence of the integration limits

means that integration is performed over the whole cross section of the beam. The energy density  $w$  of the beam electromagnetic field (1), (2) can be represented in the form

$$w = \frac{1}{16\pi} (|\mathbf{E}|^2 + |\mathbf{H}|^2) = w_\perp + w_z \quad (9)$$

where the first summand

$$w_\perp = \frac{1}{8\pi} (|u_x|^2 + |u_y|^2) = \frac{1}{4\pi} |u_x|^2 \quad (10)$$

owes to the transverse components of the field (1), and the contribution associated with the longitudinal field is

$$w_z = \frac{1}{16\pi} (|v_z|^2 + |v_{Hz}|^2) = \frac{1}{8\pi} |v_z|^2 \sim \gamma^2 w_\perp. \quad (11)$$

Our aim is to inspect the modification of the diffracted beam transverse position caused by the change of the incident beam polarization. In agreement with (9), we can separate the contributions of  $\mathbf{r}_c$  owing to the longitudinal and transverse field components:  $\mathbf{r}_c = \mathbf{r}_{c\perp} + \mathbf{r}_{cz}$  with

$$\mathbf{r}_{c\perp} = \frac{\int \mathbf{r} w_{\perp} dx dy}{\int w dx dy} \approx \frac{\int \mathbf{r} w_{\perp} dx dy}{\int w_{\perp} dx dy} = \frac{1}{I} \int \mathbf{r} |u_x|^2 dx dy \quad (12)$$

where

$$I = \int |u_x|^2 dx dy, \quad (13)$$

and

$$\mathbf{r}_{cz} = \frac{\int \mathbf{r} w_z dx dy}{\int w dx dy} \approx \frac{\int \mathbf{r} w_z dx dy}{\int w_{\perp} dx dy} = \frac{1}{2I} \int \mathbf{r} |v_z|^2 dx dy. \quad (14)$$

The second equalities in (12) and (14) are possible due to the small relative value of  $w_z$ , see (11).

The quantity (14) is the main subject of our further consideration. With knowledge of the evolution of  $v_z$  in the diffracted beam, given by (7), one can calculate the CG position in arbitrary cross section behind the screen. However, the direct calculations are difficult because the edge-diffracted beam amplitude slowly falls down at  $y \rightarrow -\infty$ , whence the integrals in (12) – (14) diverge, and special limit procedures are necessary to get meaningful results [29]. To avoid these complicated procedures, we employ the fact that in the free space, the CG of the diffracted beam evolves along a rectilinear trajectory,

$$\mathbf{r}_{cz}(z) = \mathbf{r}_{cz}(0) + \mathbf{p}_{cz} z \quad (15)$$

where  $\mathbf{p}_{cz}$  is the vector angular deviation of the CG [4,40]. To find it we consider the transformation of the paraxial beam complex amplitude on the small path between  $z=0$  and  $z=\Delta z$ ; since the law of  $v_z$  evolution (7) is identical to that of the transverse field complex amplitude (6), equation (13) of [10] permits us to write

$$v_z(x, y, \Delta z) = v_z(x, y, 0) + \frac{i\Delta z}{2k} \nabla^2 v_z(x, y, 0). \quad (16)$$

This being substituted into (14), after the integration by parts and elementary transformations supposing the complex amplitude properly behaves at  $|x|, |y| \rightarrow \infty$ , we arrive at expression (15) with  $z \rightarrow \Delta z$  in which

$$\mathbf{p}_{cz} = \frac{1}{2kI} \text{Im} \int v_z^* \nabla v_z dx dy. \quad (17)$$

Here the integration is performed across the screen plane; that is why the difference between the frames  $(x_a, y_a)$  and  $(x, y)$  (see figure 1) disappears and is no longer reflected in notation. Herewith, the integration domain only includes the ‘open’ part of the plane (in the ‘obscured’ part the function  $v_z = 0$ ) where the integrand functions behave regularly and contain no improper slowly-decreasing ‘tails’ associated with the sharp-edge diffraction. Note that equation (17), indeed, resembles the known expression for the ‘tilt’ of the CG trajectory [4,9] with the main difference that the transverse field amplitude is replaced by the longitudinal one.

#### 4. Results and discussion

Now we are in a position to make more definite estimates for a concrete experimental situation. Let the incident beam be Gaussian and the screen plane  $z = 0$  coincides with its waist plane:

$$u_x(x, y, 0) = \exp\left(-\frac{x^2 + y^2}{2b^2}\right) \quad (18)$$

where  $b$  is the waist radius measured at the  $e^{-1}$  intensity level (the constant amplitude scale factor is omitted as it does not affect the final results). For this beam, the small parameter of the paraxial approximation – the divergence angle  $\gamma$  equals to [4,10]

$$\gamma = (kb)^{-1}. \quad (19)$$

Then, according to (5),

$$v_z = -i \frac{r}{kb^2} \exp\left(-\frac{r^2}{2b^2} + i\sigma\phi\right) = -i \frac{x + i\sigma y}{kb^2} \exp\left(-\frac{x^2 + y^2}{2b^2}\right). \quad (20)$$

Hence, the characteristics of the CG position (12), (14) and (17) can be directly obtained. Corresponding integrals are to be calculated over the half-space  $(-\infty < x < \infty, a < y < \infty)$ , as in equations (6) and (7), and can be readily found.

First, we present the transverse field contributions that form the “background” for small corrections associated with the longitudinal field. The initial shift of the CG position

$$\mathbf{r}_{c\perp}(0) = bG\left(\frac{a}{b}\right) \cdot \begin{pmatrix} 0 \\ 1 \end{pmatrix} \quad (21)$$

is expectably polarization-independent and reflects the effect of partial screening of the beam cross section. Here

$$G(t) = \frac{\exp(-t^2)}{\sqrt{\pi} \operatorname{erfc}(t)} \quad (22)$$

is the function whose behavior is illustrated by figure 2;

$$\operatorname{erfc}(t) = \frac{2}{\sqrt{\pi}} \int_t^\infty \exp(-s^2) ds$$

is the complementary error function [41]. While the beam screening is small (the screen edge is situated at the far periphery of the beam intensity profile ( $a \ll -b$ ),  $G(a/b)$  is close to zero, which reflects the weak perturbation of the beam. With growing  $a$ , the CG displaces into the upper half-space, and when the beam is almost completely covered by the screen,  $a \gg b$ ,  $G(a/b)$  asymptotically tends to  $a/b$ , which means that the CG vertical coordinate practically coincides with the screen edge position  $a$ . The horizontal  $x$ -component of (21) is always zero due to the symmetry (see figure 1).

The transverse-field contribution to the trajectory tilt can be determined similarly to (17) as  $\mathbf{p}_{c\perp} = \frac{1}{kI} \operatorname{Im} \int u_x^* \nabla u_x dx dy$ ; we do not need to calculate this quantity since its  $x$ -component obviously vanishes due to the symmetry with respect to axis  $y$ , whereas the  $y$ -component appears to be zero because (18) is a real function; consequently,  $\mathbf{p}_{c\perp} = 0$ .

The contribution of the longitudinal field to the initial CG shift

$$\mathbf{r}_{cz}(0) = b\gamma^2 G\left(\frac{a}{b}\right) \cdot \begin{pmatrix} 0 \\ 1 \end{pmatrix} \quad (23)$$

shows a remarkable similarity with the main contribution (21) and, of course, preserves the same symmetry properties. The only difference is the multiplier  $\gamma^2$  reflecting the relative intensity of the longitudinal component (see (11)); in usual conditions,  $\gamma \ll 1$ , the quantity (23) supplies a very small addition to the background (21). And, at last, the most interesting result is that following from equation (17),

$$\mathbf{p}_{cz} = -\frac{\sigma}{2}\gamma^3 G\left(\frac{a}{b}\right) \cdot \begin{pmatrix} 1 \\ 0 \end{pmatrix}. \quad (24)$$

This expression (especially, its non-zero  $x$ -component) describes the main outcome of the paper. It confirms that, indeed, the diffracted beam evolution depends on the incident beam polarization, and the polarization handedness manifests itself in the tiny tilt of the diffracted beam trajectory in the direction parallel to the screen edge. This can be considered as a specific manifestation of the SHE of light in the edge-diffraction process.

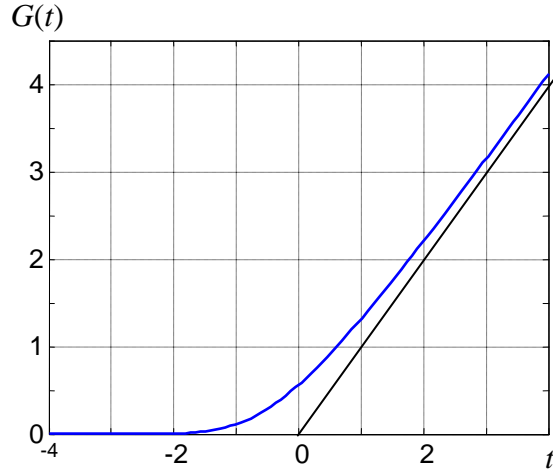


**Figure 2.** (Blue curve) Graph of the function  $G(t)$  (22); (black line) asymptote  $G = t$ .

Note that the direction of the CG shift dictated by (24) agrees with the predominant direction of the spin flow in the ‘open’ half-space (see figure 1) and reverses with the sign reversal of  $\sigma$ . This is a consequence of the origination of the CG tilt  $(p_{cz})_x$  in (24) from the longitudinal component of the incident field which is of the vortex nature (5); one can easily see that in case of the linear incident beam polarization ( $u_y = mu_x$  with real  $m$ ) this effect vanishes. The physical background of the result (24) is quite understandable. The longitudinal component (5) possesses a helical wavefront, and at a distance  $a$  from the axis its azimuthal tilt is [32]

$$\theta = \frac{2\pi/k}{2\pi a} = \frac{1}{ka} = \gamma \frac{b}{a}. \quad (25)$$

When the screen covers the central area of the beam cross section and only the peripheral part of the beam energy still propagates (see figure 1), the direction of its propagation is determined by

this wavefront tilt, i.e. the trajectory of the longitudinal component wave packet deviates in the  $x$  direction by the angle (25). Adding the multipliers responsible for the sign of the wavefront inclination,  $-\sigma$ , and for the relative “weight” of the longitudinal component (20) intensity with respect to the ‘background’ (18) intensity at the beam periphery  $r \approx a$ ,  $(\gamma a/b)^2$ , we arrive at qualitatively the same result as (24).

In fact, the diffracted beam transformation considered in this paper is almost identical to the well-known processes associated with the OV-beam diffraction [26–29,32]. But the important difference is that now these processes take place only in the small longitudinal component, which makes the result hardly perceptible and masked by the much more intensive “usual” diffraction of the non-vortex transverse components. The latter circumstances make the effect ‘per se’ extremely weak, which is emphasized by the multiplier  $\gamma^3$  in (24). However, it is geometrically isolated from other ‘background’ influences since it is the only  $x$ -directed component of the CG shift and the only CG trajectory parameter that depends on the incident beam polarization. This enables to hope that this sort of SHE can be detected in an accurate experiment, in which the polarization filtering of the transverse components as well as the polarization-selective means for detection of the longitudinal field may be profitable [15].

For example, following (15) and (24) we can estimate a possible polarization-dependent shift of the beam CG in the plane  $z$  behind the screen as  $x_c(z) = |\mathbf{p}_{cz}|z \sim \sigma\gamma^3 z$  (for a coarse approximation, all the multipliers of the order of unity are discarded). Evolution of the ‘total’ beam size in the  $x$ -direction behind the screen can be evaluated using the Gaussian beam law [39]  $b(z) = b\sqrt{1 + (z/kb^2)^2}$ , which in the far field  $z \gg kb^2$  reduces to  $b(z) \sim z/kb = \gamma z$ . Accordingly, the expectable relative CG shift due to the polarization-dependent diffraction constitutes

$$\frac{x_c(z)}{b(z)} \sim \sigma\gamma^2, \quad (26)$$

which for pretty real paraxial beams with  $\gamma \sim 10^{-2} - 10^{-3}$  seems to be a measurable effect. The situation may be even more favorable with non-paraxial, e.g., strongly focused beams with still higher  $\gamma$  although in that case the above simple theory is not fully applicable.

## 5. Conclusion

In this paper we theoretically consider the edge diffraction of a paraxial vector light beam based on the Fresnel-Kirchhoff approach and predict that the spatial pattern of the diffracted beam depends on the incident beam polarization. In particular, if the incident beam is circularly polarized, the trajectory of the diffracted beam centre of gravity experiences fine angular deviations parallel to the screen edge and reversing the sign with the polarization handedness. This effect is small but important in principle and can be considered as an additional manifestation of the spin-orbit interaction and of the spin Hall effect of light. It can be interpreted as a revelation of the internal spin energy flow associated with the spin angular momentum in circularly polarized beams and reflects the special role of the incident field longitudinal component that possesses vortex properties.

The peculiar feature of the discussed effect is that it is intimately related to the breakdown of the mirror symmetry with respect to the vertical axis (see figure 1) which is caused by the circular polarization and internal circulatory flows within the incident beam. This makes it akin

to other symmetry-breaking phenomena originating from the optical-vortex beam properties and the orbital angular momentum of the incident beam [14–17,27–29].

It should be noted that the effect considered in this paper is purely ‘geometrical’. In fact, some tiny ‘material’ modifications of the diffracted beam structure may also appear due to the difference in the screen-edge interaction with the  $x$ - and  $y$ -polarized field components. Here we did not take into account any ‘material’ factors that can affect the vector beam diffraction and, possibly, modify the numerical results. However, these will not break the symmetry discussed in the above paragraph, so the main features of the polarization-dependent beam shift described in this paper can be refined but not essentially changed. The same arguments are valid in relation to other possible improvements of the results. For example, the initial equations (1) are correct within the first order of the paraxial approximation, i.e. errors of magnitude  $\sim\gamma^2$  are possible [42], which seemingly impugns the main result (24). Nevertheless, such errors will not break the right-left symmetry in figure 1 and, anyway, the only non-symmetric term  $(p_{cz})_x$  of (24) remains untouched. Accordingly, it can be shown that a possible wavefront spherical curvature (violation of our assumption that the beam waist coincides with the screen plane) can substantially modify the initial CG position (23) as well as introduce the  $y$ -component of its angular tilt (non-zero transverse field contribution  $(p_{c\perp})_y$  and the second element  $(p_{cz})_y$  in the column vector (24)) but does not affect the first element  $(p_{cz})_x$ , which is the only important for the discussed effect.

Similarly, the use of the Gaussian beam model (18) puts no principal limitations for the final result (24); one can expect its validity (within a numerical scaling factor of the order of unity) for any axially-symmetric beam provided that the quantity  $b$  is the properly defined characteristic transverse size of the beam.

### Acknowledgement

The author is grateful to Petro Maksimyak from Chernivtsi National University, Ukraine, for stimulating ideas.

### Appendix. Orbital Hall effect in diffraction of scalar vortex beams

The diffraction of scalar OV beams was among the main motives inspiring this research (see section 1). Now we are about to perform the ‘feedback’. It looks attractive to apply some ideas of the SHE and associated instruments to the scalar diffraction problems. Here we propose to interpret the known OV-diffraction phenomena in the SHE spirit, i.e. by considering the diffracted beam trajectory in its relation to the incident beam topological charge and OAM. If, as usual, the trajectory is characterized by the CG position  $\mathbf{r}_c(z)$ , most of the above theory can be easily applied to this case.

For scalar beams, the longitudinal field component is negligible and the transverse polarization is uniform and linear so that the beam can be fully characterized by either of the transverse components (see (1)); we denote its complex amplitude simply by  $u(x, y)$ , omitting the inessential coordinate subscript. The CG is then fully determined by equations (12) and (13):

$$\mathbf{r}_c = \frac{1}{I} \int \mathbf{r} |u|^2 dx dy, \quad I = \int |u|^2 dx dy. \quad (\text{A1})$$

Then, since  $u(x, y, \Delta z)$  obeys the equation identical to (16), from (A1) one can easily derive the ‘scalar’ counterpart of (15)

$$\mathbf{r}_c = \mathbf{r}_c(0) + \mathbf{p}_c z \quad (\text{A2})$$

where

$$\mathbf{p}_c = \frac{1}{kI} \text{Im} \int u^* \nabla u dx dy \quad (\text{A3})$$

is the counterpart of formula (17), which describes the ‘orbital Hall effect’ for the diffracted scalar beam. Note that, as in (17), all integrals are calculated over the ‘open’ part of the beam cross section  $-\infty < x < \infty$ ,  $a < y < \infty$ .

As an illustration, we apply (A3) to the typical OV beam – circular Laguerre-Gaussian beam with zero radial index and topological charge  $l$  where

$$u(x, y) = (x \pm iy)^{|l|} \exp\left(-\frac{x^2 + y^2}{2b^2}\right) \quad (\text{A4})$$

(for simplicity we again suppose that the screen plane coincides with the beam waist). Substitution of (A4) into the second equation (A1) and (A4) yields

$$\mathbf{p}_c = \begin{pmatrix} p_c \\ 0 \end{pmatrix}, \quad p_c = -\frac{l}{kI} \int_{-\infty}^{\infty} dx \exp\left(-\frac{x^2}{b^2}\right) \int_a^{\infty} y (x^2 + y^2)^{|l|-1} \exp\left(-\frac{y^2}{b^2}\right) dy, \quad (\text{A5})$$

$$I = \int_{-\infty}^{\infty} dx \exp\left(-\frac{x^2}{b^2}\right) \int_a^{\infty} (x^2 + y^2)^{|l|} \exp\left(-\frac{y^2}{b^2}\right) dy. \quad (\text{A6})$$

Expectedly, the angular deviation of the diffracted beam trajectory is parallel to the screen edge and proportional to the incident OV topological charge. In case  $l = \pm 1$ , a simple analytical representation of (A5) is available:

$$p_c = \mp \gamma \frac{b}{a} \left[ 1 + \sqrt{\pi} \frac{b}{a} \text{erfc}\left(\frac{a}{b}\right) \exp\left(\frac{a^2}{b^2}\right) \right]^{-1} \quad (\text{A7})$$

where  $\gamma$  is the self-divergence angle (19) of the Gaussian envelope of the beam (A4). For example, if  $a = 0$  (the screen edge crosses the beam axis), (A7) entails  $p_c = \mp \gamma / \sqrt{\pi}$ ; this result reflects magnitude of the discussed effect: generally  $p_{cx}$  is of the order of  $\gamma$ . Asymptotically, at  $a \gg b$  expression (A7) reduces to  $p_c \approx \mp \gamma (b/a)$  which remarkably corresponds to the wavefront inclination (25). Like (24), the deviation (A7) vanishes at large negative  $a$  but, in contrast to (24), its magnitude does not grow monotonically with  $a$  and possesses a maximum  $|p_c| \approx 0.63\gamma$  at  $a \approx 0.43b$ .

For arbitrary topological charge  $l$ , explicit analytical representation of the result (A5), (A6) is cumbersome but it can be simplified in a few special situations. First, at  $a \rightarrow -\infty$  obviously  $p_c \rightarrow 0$  due to the symmetry of the internal integral in (A5); second, in the asymptotic limit  $a \gg b$  expressions (A5), (A6) can be evaluated approximately, which lead to the simple and physically transparent expression

$$p_c \approx -\frac{l}{ka} = -l\gamma \left(\frac{b}{a}\right). \quad (\text{A8})$$

Like (25), this result associates the trajectory direction with the local azimuthal tilt of the wavefront and reflects its growth with the topological charge of the OV beam. And the third solvable situation occurs at  $a = 0$  when the double integrals (A5) and (A6) can be exactly calculated in polar coordinates, and the result reads

$$p_c = -\frac{2l}{\pi kb} \frac{\Gamma\left(|l| + \frac{1}{2}\right)}{\Gamma(|l| + 1)}$$

where  $\Gamma$  is the symbol of gamma-function [41].

Of course, material of this appendix gives little addition to the accumulated knowledge of the OV beams' diffraction but it exposes some interesting aspects which, as far as we can judge, were never properly addressed in the current literature.

## References

- [1] Bliokh K Y, Niv A, Kleiner V and Hasman E 2008 Geometrodynamics of spinning light *Nature Photon.* **2** 748–53
- [2] Bliokh K Y, Ostrovskaya E A, Alonso M A, Rodríguez-Herrera O G, Lara D and Dainty C 2011 Spin-to-orbital angular momentum conversion in focusing, scattering, and imaging systems *Opt. Express* **19** 26132–49
- [3] Bliokh K Y, Rodríguez-Fortuño F J, Nori F and Zayats A V 2015 Spin-orbit interactions of light *Nature Photon.* **9** 796–808
- [4] Bekshaev A Bliokh K and Soskin M 2011 Internal flows and energy circulation in light beams *J. Opt.* **13** 053001
- [5] Liberman V S and Zel'dovich B Y 1992 Spin-orbit interaction of a photon in an inhomogeneous medium *Phys. Rev. A* **46** 5199–207
- [6] Fedoseyev V G 1991 Lateral displacement of the light beam at reflection and refraction *Opt. Spektrosk.* **71** 829–34 [*Opt. Spectr. (USSR)* **71** 483]; *Opt. Spektrosk.* **71** 992–997 [*Opt. Spectr. (USSR)* **71** 570]
- [7] Onoda M, Murakami S and Nagaosa N 2004 Hall effect of light *Phys. Rev. Lett.* **93** 083901
- [8] Bliokh K Y and Bliokh Y P 2007 Polarization, transverse shifts, and angular momentum conservation laws in partial reflection and refraction of an electromagnetic wave packet *Phys. Rev. E* **75** 066609
- [9] Bliokh K Y and Aiello A 2013 Goos–Hänchen and Imbert–Fedorov beam shifts: an overview *J. Opt.* **15** 014001
- [10] Bekshaev A Ya 2012 Polarization-dependent transformation of a paraxial beam upon reflection and refraction: A real-space approach *Phys. Rev. A* **85** 023842
- [11] Hosten O and Kwiat P 2008 Observation of the spin Hall effect of light via weak measurements *Science* **319** 787–90
- [12] Bliokh K Y 2009 Geometrodynamics of polarized light: Berry phase and spin Hall effect in a gradient-index medium *J. Opt. A: Pure Appl. Opt.* **11** 094009
- [13] Marrucci L, Manzo C and Paparo D 2006 Optical spin-to-orbital angular momentum conversion in inhomogeneous anisotropic media *Phys. Rev. Lett.* **96** 163905
- [14] Baranova N B, Savchenko A Y and Zel'dovich B Y 1994 Transverse shift of a focal spot due to switching of the sign of circular polarization *JETP Lett.* **59** 232–34
- [15] Zel'dovich B Y, Kundikova N D and Rogacheva L F 1994 Observed transverse shift of a focal spot upon a change in the sign of circular polarization *JETP Lett.* **59** 766–69
- [16] Bekshaev A 2011 Improved theory for the polarization-dependent transverse shift of a paraxial light beam in free space *Ukr. J. Phys. Opt.* **12** 10–18
- [17] Aiello A, Lindlein N, Marquardt C and Leuchs G 2009 Transverse angular momentum and geometric spin Hall effect of light *Phys. Rev. Lett.* **103** 100401

- [18] Zhao Y, Edgar J S, Jeffries G D M, McGloin D and Chiu D T 2007 Spin-to-orbital angular momentum conversion in a strongly focused optical beam *Phys. Rev. Lett.* **99** 073901
- [19] Fedoseyev V G 2001 Spin-independent transverse shift of the centre of gravity of a reflected and of a refracted light beam *Opt. Commun.* **193** 9–18
- [20] Fedoseyev V G 2008 Transformation of the orbital angular momentum at the reflection and transmission of a light beam on a plane interface *J. Phys. A: Math. Theor.* **41** 505202
- [21] Bekshaev A Ya and Popov A Yu 2002 Method of light beam orbital angular momentum evaluation by means of space-angle intensity moments *Ukr. J. Phys. Opt.* **3** 249–57
- [22] Dasgupta R and Gupta P K 2006 Experimental observation of spin-independent transverse shift of the centre of gravity of a reflected Laguerre-Gaussian light beam *Opt. Commun.* **257** 91–96
- [23] Bekshaev A Ya 2009 Oblique section of a paraxial light beam: criteria for azimuthal energy flow and orbital angular momentum *J. Opt. A: Pure Appl. Opt.* **11** 094003
- [24] Bekshaev A 2011 Role of azimuthal energy flows in the geometric spin Hall effect of light (arXiv:1106.0982)
- [25] Marienko I G, Vasnetsov M V and Soskin M S 1999 Diffraction of optical vortices *Proc. SPIE* **3904** 27–34
- [26] Masajada J 2000 Half-plane diffraction in the case of Gaussian beams containing an optical vortex *Opt. Commun.* **175** 289–94
- [27] Arlt J Handedness and azimuthal energy flow of optical vortex beams 2003 *J. Mod. Opt.* **50** 1573–80
- [28] Cui H X, Wang X L, Gu B, Li Y N, Chen J and Wang H T 2012 Angular diffraction of an optical vortex induced by the Gouy phase *J. Opt.* **14** 055707
- [29] Bekshaev A Ya, Mohammed K A and Kurka I A 2014 Transverse energy circulation and the edge diffraction of an optical-vortex beam *Appl. Opt.* **53** B27–37
- [30] Bekshaev A and Mohammed K A 2013 Transverse energy redistribution upon edge diffraction of a paraxial laser beam with optical vortex *Proc. SPIE* **9066** 906602
- [31] Bekshaev A Ya and Mohammed K A 2015 Spatial profile and singularities of the edge-diffracted beam with a multicharged optical vortex *Opt. Commun.* **341** 284–94
- [32] Bekshaev A Ya, Kurka I A, Mohammed K A and Slobodeniuk I I 2015 Wide-slit diffraction and wavefront diagnostics of optical-vortex beams *Ukr. J. Phys. Opt.* **16** 17–23
- [33] Bekshaev A Ya and Soskin M S 2007 Transverse energy flows in vectorial fields of paraxial beams with singularities *Opt. Commun.* **271** 332–48
- [34] Berry M V 2009 Optical currents *J. Opt. A: Pure and Applied Optics* **11** 094001
- [35] Bekshaev A Y 2013 Subwavelength particles in an inhomogeneous light field: Optical forces associated with the spin and orbital energy flows *J. Opt.* **15** 044004
- [36] Bliokh K Y, Bekshaev A Y and Nori F 2013 Dual electromagnetism: helicity, spin, momentum and angular momentum *New J. Phys.* **15** 033026
- [37] Bliokh, K Y and Nori F 2015 Transverse and longitudinal angular momenta of light. *Phys. Reports* **592** 1–38
- [38] Antognozzi M, Bermingham C R, Harniman R L, Simpson S, Senior J, Hayward R, Hoerber H, Dennis M R, Bekshaev A Y, Bliokh K Y and Nori F 2016 Direct measurements of the extraordinary optical momentum and transverse spin-dependent force using a nano-cantilever *Nat. Phys.* **12** 731–35
- [39] Anan'ev Yu A 1992 *Laser Resonators and the Beam Divergence Problem* (Bristol, Philadelphia and New York: Adam Hilger)

- [40] Anan'ev Yu A and Bekshaev A Ya 1994 Theory of intensity moments for arbitrary light beams *Opt. Spectr.* **76** 558–68
- [41] Abramovitz M and Stegun I 1964 *Handbook of mathematical functions* (National Bureau of standards, Applied mathematics series, 55)
- [42] Lax M, Louisell W H and McKnight W B 1975 From Maxwell to paraxial wave optics *Phys. Rev. A* **11** 1365–70